3-D CONSTRAINT EFFECTS ON FRACTURE MECHANICS SPECIMENS

Emerson Giovani Rabello
Centro de Desenvolvimento da Tecnologia Nuclear - CDTN/CNEN. Caixa Postal 941, CEP 30123-970, Belo Horizonte, MG, Brasil.
egr@cdtn.br

Miguel Mattar Neto
Instituto de Pesquisas Energéticas e Nucleares - IPEN/CNEN. Caixa Postal 11049, CEP 05422-970, São Paulo, SP, Brasil.
mmattar@ipen.br

Julio Ricardo Barreto Cruz
Distrito de Fortaleza - DIFOR/CNEN. Av. Antonio Sales, 1418, CEP 60135-101, Fortaleza, CE, Brasil.
jrcruz@cnen.gov.br

Paulo de Tarso Vida Gomes
Centro de Desenvolvimento da Tecnologia Nuclear - CDTN/CNEN. Caixa Postal 941, CEP 30123-970, Belo Horizonte, MG, Brasil.
gomespt@cdtn.br

Abstract. *The constraint is accepted as a measure of the triaxiality level at the crack-tip. Specimens with different a/W ratios present variation on the stress field ahead of the crack-tip. A stress relaxation can occur depending on the a/W values which is known as loss of constraint and has strong influence on the structural steels fracture toughness.*
Different approaches have been proposed to quantify constraint and to describe the effects of constraint variations on engineering fracture toughness characterized by J-integral, or equivalently the crack-tip opening displacement, CTOD. This paper presents the results of a numerical investigation, in which single-edge cracked bars in three point bend SE(B) and compact tension C(T) specimens, with different relative crack lengths, were systematically studied via detailed three-dimensional finite element analyses. A new parameter is then proposed to quantify crack-tip constraint.

Keywords*: J-integral, Crack-tip constraint, Q-Parameter, Finite-Elements Analysis (FEA).*

1. Introduction

A fundamental assumption of fracture mechanics is that the crack-tip conditions can be uniquely characterized by a single parameter: the stress intensity factor *K* (or *J*-integral). When this assumption is valid, the critical value of the crack-tip parameter represents a size independent measure of the fracture toughness. This situation occurs in small-scale yielding (*SSY*) conditions, when the plastic zone size remains small compared to the specimen external geometry. However, for large-scale yielding (*LSY*) in finite bodies, the relationship between the scaling parameter (i.e. *J*-integral), and the near-tip fields loses the one-to-one correspondence. This loss of uniqueness (also called: loss of constraint) produces an increases in the fracture toughness, observed in tension geometries and shallow notch bend specimens.

Different approaches have been proposed to quantify constraint and to describe the effects of constraint variations on engineering fracture toughness characterized by J-integral (or equivalently the crack-tip opening displacement, *CTOD*). The *J-Q* methodology developed by O'Dowd and Shih (1991, 1992) is one of the main theories used to describe the constraint effects in fracture toughness. In this methodology, the *J*-integral sets the size scale over which large deformations and high stresses are developed, while the additional parameter (*Q*) quantifies the level of stress triaxiality ahead of the crack-tip. Under increased loading, each fracture specimen follows a characteristic driving force curve, or trajectory, which defines the evolution of crack-tip deformation (*J*) and constraint (*Q*).

This paper presents the results of a numerical investigation, in which single-edge cracked bars in three point bend *SE(B)* specimens and compact tension *C(T)* specimens, with different relative crack lengths, were systematically studied using detailed three-dimensional finite element analyses. A new parameter is then proposed to quantify crack-tip constraint in three dimensional cases.

2. *J-Q* Methodology

The *J-Q* description for plane-strain crack-tip fields (mode I) derives initially from consideration of the boundary layer model for small-scale yielding (*SSY*). Crack-tip stresses for linear elastic conditions have the form shown in Eq. (1) (Willians, 1957):

$$\sigma_{ij} = \frac{K_I}{\sqrt{2\pi r}} f_{ij}(\theta) + T\,\delta_{1i}\cdot\delta_{1j} \tag{1}$$

where: r and θ are polar coordinates centered at the crack-tip (θ = 0°); K_I is a Stress Intensity Factor; δ_{ij} is the Kronecker delta, E is a Young's Modulus and ν is Poisson's Ratio.

Crack-tip fields differing in stress triaxiality are generated by varying the non-singular stress, T, parallel to the crack plane. In the computational model for *SSY*, the conditions defined by Eq. (1) are imposed incrementally on the remote outer boundary of a symmetrically constrained semi-circular mesh of elements focused on the crack-tip.

O'Dowd and Shih (1991, 1992) employed asymptotic analyses and detailed finite element analyses to propose the approximate two-parameter description of the crack-tip fields which may be applied under small and large-scale yielding conditions:

$$\sigma_{ij} = \sigma_0 f_{ij}\left(\frac{r}{J/\sigma_0}, \theta, Q\right) \qquad \varepsilon_{ij} = \varepsilon_0 g_{ij}\left(\frac{r}{J/\sigma_0}, \theta, Q\right) \tag{2}$$

The dimensionless second parameter, Q, in Eq. (2) defines the amount by which σ_{ij} and ε_{ij} in fracture specimens differs from the adopted *SSY* reference solution at the same applied J.

To a good approximation, O'Dowd and Shih (1991, 1992) showed that $Q\sigma_0$ represents the difference in hydrostatic stress over the forward sector ahead of the crack-tip between the *SSY* conditions and fracture specimen fields. Thereby, operationally, Q is defined by:

$$Q \equiv \frac{\sigma_{\theta\theta} - (\sigma_{\theta\theta})_{SSY}}{\sigma_0}, \quad at\ \theta = 0, \quad r = 2J/\sigma_0 \tag{3}$$

The specimen stresses ($\sigma_{\theta\theta}$) in Eq. (3) are evaluated from finite element analyses containing sufficient mesh refinement to solve the field at this length scale ($r = 2J/\sigma_0$).

At low deformation levels, fracture specimens experience *SSY* conditions and Q remains very close to zero. Once large-scale yielding conditions prevail, hydrostatic stresses at the crack-tip are substantially smaller than those in *SSY* at the same J-value. This difference produces negative Q values once the specimen deviates from *SSY* conditions. For deeply notched *SE(B)* and *C(T)* specimens, the elastic T-stress is positive and thus Q takes on slightly positive values at low deformation levels before constraint loss occurs.

3. Extension of *J-Q* Methodology

The previously presented *J-Q* Methodology was developed for the plain strain conditions, exclude the effect of the specimens thickness. Taking account of the great variation of *Q*-Parameter to the extent of the crack front, a new approach for considering of the thickness effects on the loss of constraint may be used.

Thus, based in the concept of "functional integration", used in the development of the domain integral (Koppenhoefer et al., 2002; Moran & Shih, 1987), the conventional *J-Q* Trajectories can be extended including the thickness effects. According to this concept, all integrals of continuous functions can be expressed for the addition of the values on a domain, duly normalized, to supply a functional average value.

A domain can be defined by a domain function or by a weight function ($w(x)$) that it is equal the zero outside it and equal a determined value inside it. The average value of a function ($F(x)$) on this domain can be written as:

$$\frac{\int F(x) \cdot w(x) dx}{\int w(x) dx} = \overline{F} \tag{4}$$

Considering the crack representation shown in the Fig. 1 and the application of the the domain integration concept a new parameter can be established (Q_A) to represent the effect of the loss of constraint at the crack-tip:

$$Q_{A(B_{z=0} \to B_{z=1})} = \frac{\int_{B_{z=0}}^{B_{z=1}} Q(z) \cdot w(z) dz}{\int_{B_{z=0}}^{B_{z=1}} w(z) dz} = \frac{\overline{Q}}{A_w} \tag{5}$$

Where: $Q(z)$ is the *Q*-Parameter value in each point to the extent of the thickness (z-axis); A_W is the area below the curve of the domain function ($w(z)$) in which *Q*-function was integrated, and $\overline{Q}$ is the *Q*-Parameter average, determined to the extent of the specimen thickness.

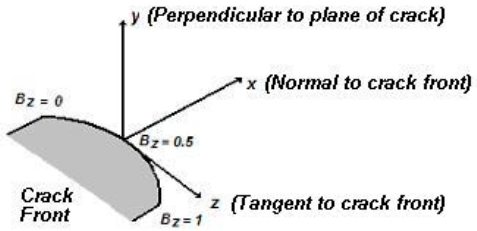

Figure 1. 3D-Crack representation

As in the case of the domain integral, for straight through thickness cracks, the domain function is constant and uniform to the extent of the thickness. Thus, physically Q_A-Parameter is associated with an average hydrostatic stress, that represents the stress triaxiality (constraint level) of a studied geometry.

4. Numerical analyses

The studied specimens are presented in Fig. 2, where crack length, width and thickness are denoted by *a*, *W* and *B*. In terms of in-plane constraint, two different values of *a/W* are considered: 0.100, and 0.500.

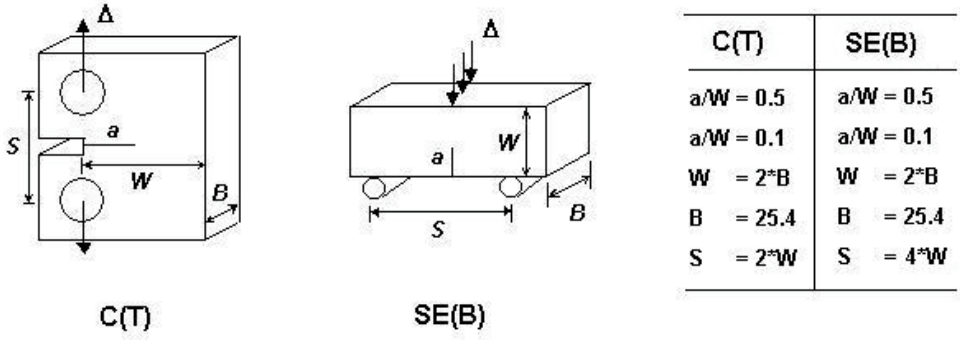

C(T)	SE(B)
a/W = 0.5	a/W = 0.5
a/W = 0.1	a/W = 0.1
W = 2*B	W = 2*B
B = 25.4	B = 25.4
S = 2*W	S = 4*W

Figure 2. Studied specimens

Figure 3 depicts typical 3-D FE meshes, employed in the present work. Finite Elements meshes typically have about 12000 elements (8-node hexahedron elements). Symmetry conditions are fully utilized for efficient computation which enable the use of one-quarter models as indicated. Ten layers of elements had been used across the thickness to capture the stress gradient in this direction.

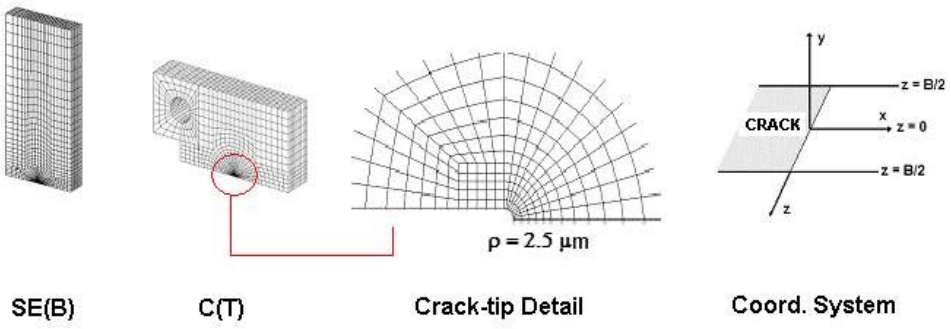

Figure 3. 3D-Models for finite elements analyses

The uniaxial stress-strain curve follows a power-law given by Ramberg-Osgood equation:

$$\frac{\varepsilon}{\varepsilon_0}=\frac{\sigma}{\sigma_0} \qquad \varepsilon \le \varepsilon_0 ; \quad \frac{\varepsilon}{\varepsilon_0}=\left(\frac{\sigma}{\sigma_0}\right)^n \qquad \varepsilon > \varepsilon_0 \tag{6}$$

where: ε_0 and σ_0 define limits for the initial linear portion of the response. All computations use E/σ_0 = 500, Poisson's ratio ν = 0.3 and "*n*" = 5.

Finite elements results were obtained with the computer code WARP3D (Koppenhoefer et al., 2002). This code uses an incrementally iterative Newton procedure to solve the nonlinear equilibrium equations.

To alleviate the severe volumetric locking under incompressible plastic deformation in the conventional 8-node hexahedron element , WARP3D code adopts the *B-bar* modification suggested by Hughes (1980).

The local energy release rate for Mode I crack extension at each point along the front is given by:

$$J = \lim_{\Gamma \to 0} \int_{\Gamma} W\ n_1 - \sigma_{ij} \frac{\delta\, u_i}{\delta\, x_1} n_j\ d\ \Gamma \tag{7}$$

Where: W denotes the strain-energy density, Γ is a closed boundary over a plane normal to the crack front, n is a unit normal vector to Γ, σ_{ij} and u_i are the stress tensor components in the Cartesian coordinates system localized in the crack front

In the present analyses, numerical evaluation of Eq. (7) is accomplished with a domain integral method (Shih et al., 1986) as implemented in WARP3D. The resulting formulation provides pointwise values of J in the extent of the crack front at each thickness layer and a thickness averaged value at each loading level.

The Q-Parameter was obtained along the thickness using the JQCRACK program (Cravero and Ruggieri, 2003). The *SSY* reference fields required for Q computations are obtained from plane-strain, finite element solutions of the modified boundary layer model of an infinite body, single-ended crack problem (Al-Ani and Hanford, 1991).

5. Results and discussion

The Q-Parameter values int the extent of the thickness (normalized by B_x/B_T, where B_T is the total thickness) are presented in the Fig. 4 and Fig. 5. It was observed that the Q-Parameter values decrease strongly along the thickness. This effect becomes more pronounced for higher loads.

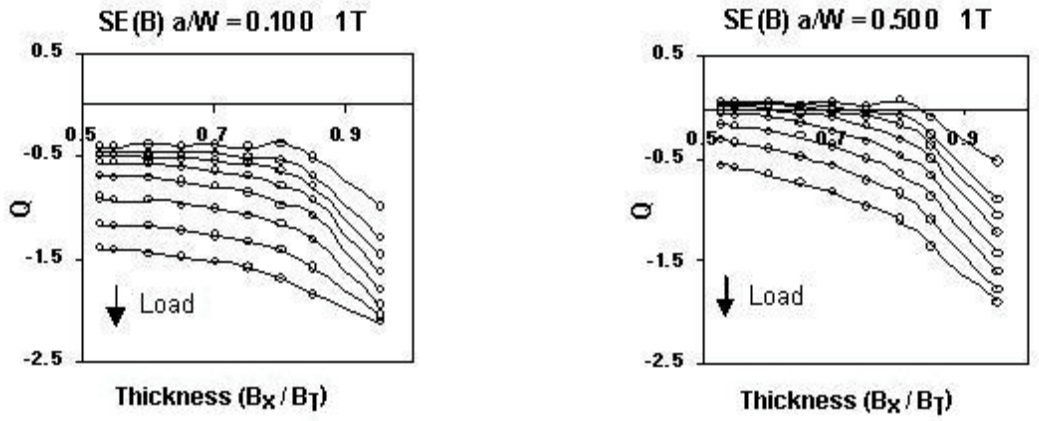

Figure 4. Q vs. Thickness - *SE(B) a/W* = 0.1 and 0.5

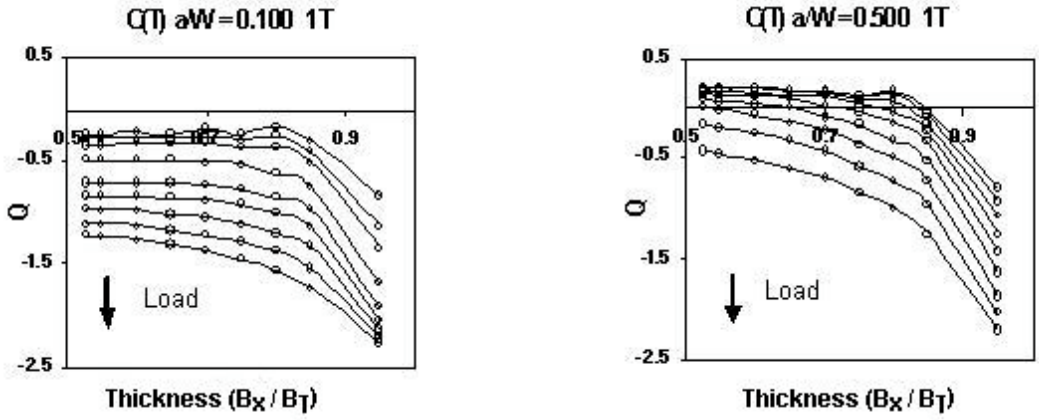

Figure 5. Q vs. Thickness - *C(T) a/W* = 0.1 and 0.5

The *Q*-Parameter decreases in the extent of the thickness reveal the in-plane and out-of-plane constraint effects in the specimens. Thereby, the extension of the *J-Q* Methodology (shown in item 3) may be used to characterize the constraint effects along the thickness.

Figures 6-7 show the *J-Q* Trajectories for all the studied geometries. The lines correspond to the results obtained for the plane-strain condition (denoted by Q_{PS}). The dotted-lines represent the *J*-Q_A Trajectories (*J-Q* Trajectories corrected with the Q_A-Parameter). The *J*-Integrals values were normalized for $J/b\sigma_0$, where *b* is the ligament (*W* - *a*) and σ_0 is the yield strength of the material (400 MPa).

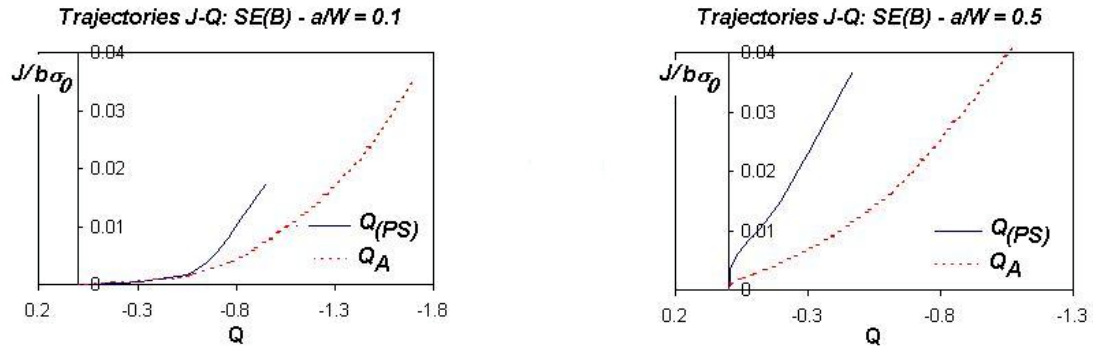

Figure 6. *J-Q* Trajectories - *SE(B) a/W* = 0.1 and 0.5

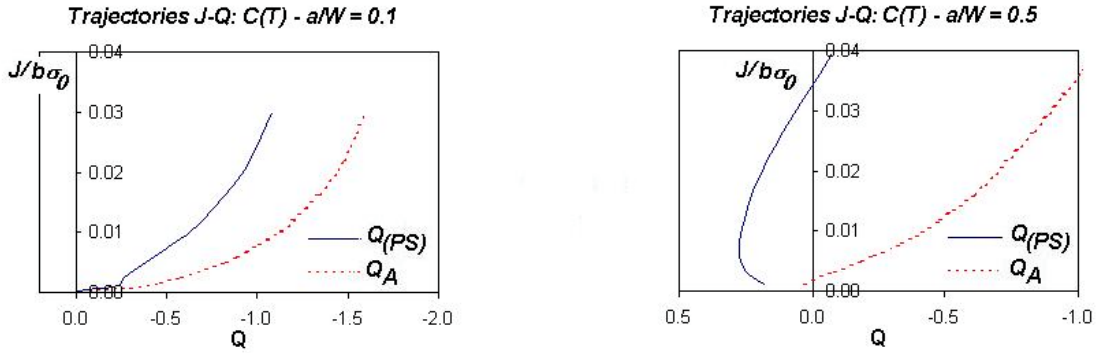

Figure 7. *J-Q* Trajectories - *C(T) a/W* = 0.1 and 0.5

For all studied specimens, the constraint effects are larger for the shallow cracks. It is noticed that for sizes crack (denoted by the relationship *a/W*) smaller than 0.5, the values of *Q* are negative, meaning that the specimen suffers a strong loss of constraint.

C(T) specimens with deep cracks (*a/W* = 0.5) present minor loss of constraint that the studied bending geometries. This fact can be observed in the side where the *Q*-values are positive, presented in Fig. 7.

The *J*-Q_A Trajectories describe the constraint behavior in an efficient way, showing agreement with the constraint effects in relation to the crack sizes of the specimens. However, the displacement of the *J*-Q_A Trajectories in relation to the *J-Q* Trajectory indicates a decrease in the fracture toughness values.

6. Conclusions

The developed analyses evidence the importance of the constraint effects on the materials fracture toughness. Also, the use of the biparametric methodology (*J-Q*) seems to be quite efficient in the assessment of the constraint effects.

The introduction of a new Q_A-Parameter to evaluate the constraint effects, gives a better understanding of those effects, including the effects of the specimen thickness in its formulation. This parameter propitiates a better knowledge on the in-plane and out-of-plane constraint effects.observed in experimental data.

7. References

Al-Ani, A.M., Hancock, J.W., 1991. J-dominance of short cracks in tension and bending. Journal of Mechanics and Physics of Solids, vol. 39, pp. 23-43.

Cravero, S., Ruggieri, C., 2003. JQCRACK Versão 1.0 Cálculo numérico do parâmetro hidrostático Q para componentes estruturais 2D contendo trinca. Boletim Técnico da Escola Politécnica da Universidade de São Paulo - BT/PNV/59, Departamento de Engenharia Naval e Oceânica.

Huges, T.J., 1980. Generalization of selective integration procedures to anisotropic and nonlinear media. International Journal for Numerical Methods in Engineering, vol. 15, pp. 1413-1418.

Koppenhoefer, K., Gullerud, A., Roy, A., Walters, M., Dodds, R. H., 2002. WARP3D-Release 14.1: 3D Dynamic nonlinear fracture analysis of solids using parallel computers and workstations. Structural Research Series 607. UILU-ENG-95-2012, University of Illinois at Urbana-Champaign.

O'Dowd, N.P., Shih, C.F., 1991. Family of crack-tip fields characterized by triaxiality parameter: Part I – Structure of fields. Journal of the Mechanics and Physics of Solids, vol. 39, n. 8, pp. 989-1015.

O'Dowd, N.P., Shih, C.F., 1992. Family of crack-tip fields characterized by triaxiality parameter: Part II – Structure of fields. Journal of the Mechanics and Physics of Solids, vol. 40, pp. 939-963.

Shih, C.F., Moran, B., & Nakamura, T., 1986. Energy release rate along a three-dimensional crack front in a thermally stressed body. International Journal of Fracture, vol. 30, pp. 79-102.

Willians, M.L., 1957. Journal of Applied Mechanics, vol. 24, pp. 109-114.

8. Responsibility notice

The authors are the only responsible for the printed material included in this paper.